

# Performance Evaluation of an ANC-based Hybrid Algorithm for Multi-target Wideband Active Sonar Echolocation System

Jason Chien-Hsun Tseng

**Abstract**—This paper evaluates performances of an adaptive noise cancelling (ANC) based target detection algorithm on a set of real test data supported by the Defense Evaluation Research Agency (DERA UK) for multi-target wideband active sonar echolocation system. The hybrid algorithm proposed is a combination of an adaptive ANC neuro-fuzzy scheme in the first instance and followed by an iterative optimum target motion estimation (TME) scheme. The neuro-fuzzy scheme is based on the adaptive noise cancelling concept with the core processor of ANFIS (adaptive neuro-fuzzy inference system) to provide an effective fine tuned signal. The resultant output is then sent as an input to the optimum TME scheme composed of two-gauge trimmed-mean (TM) levelization, discrete wavelet denoising (WDeN), and optimal continuous wavelet transform (CWT) for further denoising and targets identification. Its aim is to recover the contact signals in an effective and efficient manner and then determine the Doppler motion (radial range, velocity and acceleration) at very low signal-to-noise ratio (SNR). Quantitative results have shown that the hybrid algorithm have excellent performance in predicting targets' Doppler motion within various target strength with the maximum false detection of 1.5%.

**Keywords**—Wideband Active Sonar Echolocation, ANC Neuro-Fuzzy, Wavelet Denoise, CWT, Hybrid Algorithm.

## I. INTRODUCTION

**R**ECOVERING active acoustic sonar returns in multipath media is a core problem of underwater signal processing to detect and classify underwater targets. Because the system is concerned with estimation of targets' motion parameters, it is well known that the implementation of such system exploits the time-scale joint representation of target echoes [1]. The technique used to measure time and scale of objects is commonly known as the cross correlation or matched filter processing [2]. As in the wideband environment, this technique estimates the time-delay and scale-change by cross correlation of overlapping segments of the received complex signal with a set of basis functions matched to the transmitted signal. This method is then referred to as wideband replica correlation (WRC). The standard WRC processing works well for the most problems and has optimum performance with the noise-free signal or the maximum output signal-to-noise ratio (SNR) condition [3]. In the presence of severe interference or in highly distorting media such as spread or multipath channels [4], the WRC processing, however, degrades the underlying back scattering returns. Together with the system characteristics such as beam patterns and

Jason Chien-Hsun Tseng is with the Department of Information Engineering Kun Shan University, Taiwan email: jt571029@mail.ksu.edu.tw.

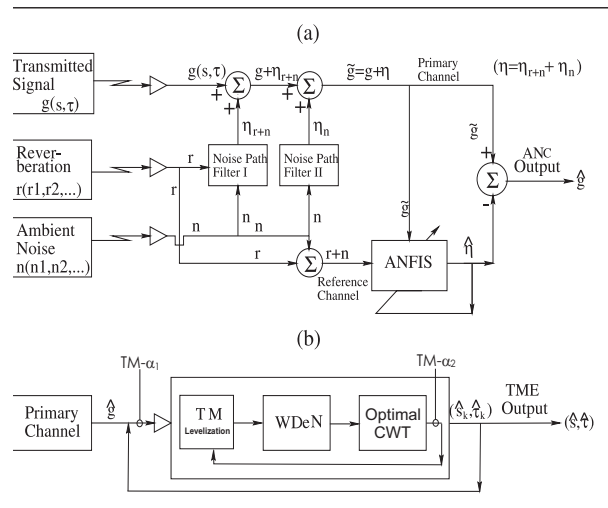


Fig. 1. A block diagram of the ANC-TME hybrid algorithm. (a) adaptive ANC neuro-fuzzy scheme. (b) Iterative TME scheme.

transmitted signal, the severe interference has made the detection even more difficult. This is because sharp peaks are more sensitive to a sidelobe correlation interference mainly arising from unwanted harmonics of the transmission, which correlate with the replica. This assertion is even more justified for harmonic ghosts being generated by overlapping these unwanted harmonics after reflection from the first break (the interface between the surface of the earth formation and the covering water) with the weak reflections from deep reflecting interfaces [4].

A fast hybrid denoising algorithm [5], [6], [7] based on an ANC neuro-fuzzy processor and optimal wavelet transforms is proposed for multi-target wideband active sonar echolocation system for which one or more underwater target returns are masked by interference. The aim of the hybrid algorithm proposed is to recover the contact signals in an effective and efficient manner and then determine the Doppler motion parameters (radial range, velocity and acceleration) at various target strength of SNR. Together with the real data set supported by the DERA UK, the hybrid algorithm is tested for its performance in terms of targets' motion detection based on Doppler time-scale and time-delay of the received echo via matched optimal filtering mechanisms (i.e. training sets). The detection process of the hybrid algorithm as illustrated

in Fig. 1 is composed of two distinctive schemes: adaptive ANC neuro-fuzzy scheme and iterative optimum target motion estimation (TME) scheme. The adaptive ANC neuro-fuzzy scheme depicted in Fig. 1(a) is based on the adaptive noise cancelling concept [8] with the core processor of ANFIS (adaptive neuro-fuzzy inference systems [9]), while the iterative optimum TME scheme depicted in Fig. 1(b) is based on the optimal wavelet transforms with multilevel threshold denoising. Using the adaptive learning intelligent systems, unwanted parts of the target returns including harmonic ghosts and those interference/noise contained in the higher frequency ranges are removed, and hence to effectively improve the target strength. We note that a priori the echo signals of interest are in the lower frequency ranges. The stage of noise cancelling exploits capabilities of ANFIS in tracking both linearity and nonlinearity in multidimensional input space and thus alleviating the sidelobe correlation interference.

The resultant signal is then proceeded by the iterative optimum TME scheme for further localizing potentials and then recovering the contact signal via matched filtering mechanisms. Process steps include: two-gauge trimmed-mean (TM) levelization, discrete wavelet denoising (WDeN) [10], and optimal CWT operation via FIR filtering structure. More specifically, the TM-levelization step is a dynamic level-based process controlled by two gauges not only to keep updating the TME scheme but also to remove power of most excessive sharp detail in the sense of trimmed mean estimation. Following from the TM step, the WDeN step associated with an octave subband decomposition is applied. Its functionality is to further suppress the remaining noise part of the training data and thus produce fine tuned test cells for the final step of target mapping, the optimal CWT operation via FIR matched filtering mechanisms (i.e. training sets). Here the similarity measurement in terms of CWT signal mapping is optimized in the scale domain by the combination of golden section search and successive parabolic interpolation method [11]. By combining the adaptive ANC neuro-fuzzy scheme in the first place with the iterative optimum TME scheme, the ANC-TME hybrid algorithm is developed for real-time applications in DSP-FPGA hardware implementation. It's task is to rapidly and accurately processing targets' echoes in the presence of severe interference, a combination of backscattered reverberation and ambient noise. Quantitative analysis of the evaluation results have shown that the hybrid algorithm not only meets the development requirements but also provides a higher degree of signal detection capability with an increased robustness against false signal detections.

## II. REVIEW OF TECHNIQUES

### A. WRC processing and optimum detection algorithm

Let us consider wideband signals in a multiple nondirectional sonar channels for which the received waveform  $\tilde{g}(t)$  can be described mathematically as [2]

$$\tilde{g}(t) = \sum_{i=1}^I \alpha_i g_i(t) + \eta(t). \quad (1)$$

This model accounts for superposition of contact signal known as target signatures  $g_i(t)$  as in Eq. (2), which are received

Doppler distorted pulses in the  $L^2(\Omega)$  Hilbert Space of finite energy at time  $t \in \Omega \subset \mathbb{R}$ . Furthermore, the background interference  $\eta(t)$  as in Eq. (3) involves reverberation waveform  $r(t)$  and additive ambient noise  $n(t)$ :

$$g_i(t) = \sqrt{S_i} \psi(S_i(t - D_i)) \quad (2)$$

$$\eta(t) = \tilde{h}(t) * r(t) + n(t) \quad (3)$$

Here parameters are defined by  $\psi$  the transmitted signal (pulse),  $\alpha_i$  amplitude (attenuation value) for the  $i^{th}$  echo,  $S_i$  true Doppler scale for the  $i^{th}$  echo,  $D_i$  true round-trip time-shift for the  $i^{th}$  echo,  $\tilde{h}$ , an unknown channels of arbitrary noise path filter. Reverberations due to multiple reflection from the medium boundaries including the surface, volume and bottom usually contribute in varying proportions. The common scenario is chosen for which the sonar devices are assumed to be mounted either on a surface ship or underwater submarine [12]. As a result, the scattering process and the dependence of the received reverberation on range can be modelled in terms of having an intensity with exponential statistics or an envelope, a square root of the intensity, with the Rayleigh statistic. The probability density function of the reverberation model is then given by

$$\rho(\gamma|\sigma) = \frac{\gamma}{\sigma^2} e^{-\gamma^2/2\sigma^2} \quad (4)$$

where  $\gamma$  is the amplitude of the envelope and  $\sigma$  is the standard deviation representing the expected level of intensity. The aim of the model in Eq. (1) is to isolate specular returns from the background interference by using the wideband replica correlation. Hence, a pair of scale-time joint motion parameters  $(\hat{S}_i, \hat{D}_i)$  associated with the  $i^{th}$  return can then be estimated by solving the maximization problem of the wideband ambiguity function  $WC_{\psi\tilde{g}}(s, \tau)$  over both parameters simultaneously:

$$\max_{s.t. (s>0, \tau \in \mathbb{R})} \{ ||WC_{\psi\tilde{g}}(s, \tau)||^2 \} = ||WC_{\psi\tilde{g}}(s^*, \tau^*)||^2. \quad (5)$$

Here  $WC_{\psi\tilde{g}}(s_i, \tau)$  associated with the  $i^{th}$  specular return having the Doppler scale  $s_i$  is defined as

$$WC_{\psi\tilde{g}}(s_i, \tau) = \int_{-\infty}^{\infty} \tilde{g}(t) \overline{\psi_{s_i}(t - \tau)} dt = \langle \tilde{g}, \psi_{s_i}(t - \tau) \rangle \quad (6)$$

which utilizes  $\psi_{s_i}(t) \equiv \sqrt{s_i} \psi(s_i t)$  as a template to form the hypothetical signal. As a result, the  $i^{th}$  element of optimum can be found by  $s_i^* = \hat{S}_i \approx \varepsilon S, \varepsilon > 0$  and  $\tau_i^* = \hat{D}_i \approx D$ . Due to computational expensive as two decision variables involved and encountering difficulties in dealing with severe interference [4], it suggests to consider basis functions  $\psi_{s,\tau}(t)$  already appeared as wavelets. Provided the variable change  $s \mapsto \frac{1}{s}$ , the inner product of WRC used as a similarity measurement is then a CWT of  $\tilde{g}(t)$  with respect to  $\psi(t)$  [10]. Consequently, the aim of echolocation detection may be solved by seeking the local maximum of CWT coefficients:

$$\max_{s>0, \tau \in \mathbb{R}} \{ ||CWT_{\psi\tilde{g}}(s, \tau)||^2 \}. \quad (7)$$

Given time support  $t \in [0, T]$  for  $\tilde{g}(t)$ , a discrete-time version of the CWT consists of dividing the time interval into  $N$  sub-intervals, and approximating the input signal as  $\tilde{g} \equiv [\tilde{g}(t_0), \dots, \tilde{g}(t_{N-1})]$  where  $t_k = (k+1) \frac{T}{N}$ . The discrete

CWT coefficients obtained for the sampled input signal  $\tilde{g}$  at the scale  $s$  can be represented by a bank of FIR filter output response with filter coefficients  $h(s, \ell)$  [5], i.e.,

$$\begin{aligned} CWT_{\psi} \tilde{g}[s, k] &= y[s, k] = h(s, k) * \tilde{g}(k) \\ &= \sum_{\ell=\max\{0, k-L\}}^{\min\{k, n-1\}} h(s, \ell) \tilde{g}(k - \ell), \end{aligned} \quad (8)$$

for  $k = 0, \dots, n + L - 2$ . Here the filter tap range, due to the symmetric structure of the mother wavelet, is setting as

$$\frac{[-sT_{\psi}, sT_{\psi}]}{sT_{\psi}} (2T_{\psi} f_{\psi} - 1) \equiv [0, L - 1] \quad (9)$$

with sampling rate  $f_{\psi}$  and effective support  $[-T_{\psi}, T_{\psi}]$  of the mother wavelet  $\psi$ . Due to the discrete setting by the FIR filtering occurred in the abscissa time-domain, a pair of optimizers ( $s^*, \tau^*$ ) can be evaluated using the following optimal target training and mapping algorithm [5]:

*Algorithm 2.1:* Set  $i = 1$ . Let us denote

$$\sum_{k=\lfloor \frac{s}{2} \rfloor}^{\lfloor \frac{2N+L}{2} \rfloor} |\hat{y}[s, k]|^2 \equiv f(s) \quad (10)$$

where  $\hat{y}[s, k] = h(s, k) * \hat{g}(k)$  and  $\hat{g}$  is a denoised signal of  $\tilde{g}$ . Denote  $f^n(s), n = 1, 2, \dots$  by the  $n$ -th derivative of  $f(s)$ . Define  $\epsilon > 0$  and parameters  $s_0, s_{min}, s_{max}$  as CWT reference scales corresponding to the Doppler scales  $\tilde{s}_0, \tilde{s}_{min}, \tilde{s}_{max}$  which represent the stationary, minimum and maximum target motions, respectively. Let  $k_0, k_{min}, k_{max}$  be time indices corresponding to the Doppler scales  $\tilde{s}_0, \tilde{s}_{min}, \tilde{s}_{max}$ , respectively.

- 1) Given parameters  $s_0, s_{min}, s_{max}$ , find an optimizer  $\hat{s}_i^*$  that maximizes  $f(s)$ , i.e.,

$$\hat{s}_i^* = \arg \max_{s>0} f(s). \quad (11)$$

- 2) Knowing the scale  $\hat{s}_i^*$ , the corresponding time-delays  $\hat{\tau}_{i,j}^{*n} = \hat{\tau}_i^*(k_j^n), j = 1, 2, \dots$  can be obtained for which indices  $k_j^n$  are given by

$$k_j^n = \arg \max_{(n,k)} \{|f_k^n(\hat{s}_i^*) - f_k(\hat{s}_i^*)|\} \quad (12)$$

where functions  $f_k^n$  and  $f_k$  are denoted by the  $k^{th}$  sample of the functions.

- 3) Let  $var(f)$  be the variance of the values in  $f$ . If the stopping criteria

$$\max(var(f_k^n(\hat{s}_i^*))) \geq \max(var(\eta(t_i))) \quad (13)$$

$$\frac{|k_j^n - k_0|}{\max\{|k_{min} - k_0|, |k_{max} - k_0|\}} < 1 \quad (14)$$

are satisfied, then stop and set  $(s^*, \tau^*) = (\hat{s}_i^*, \hat{\tau}_i^*(k_j^n))$ ; otherwise return to Step 1) with index  $i$  replaced by  $i+1$ .

### B. ANFIS learning, TM-levelization and Wavelet Denoising operations

- ANFIS: The adaptive network represented by the ANFIS architecture [9] is based on the Sugeno's fuzzy if-then rule [13] for which the fuzzy reasoning mechanism is derived for an output  $\eta$  from a given input training data set  $n(t)$ . In theory, the network is combined with the gradient descent and least-squares methods. The gradient descent method is in the forward path to upgrade the

premise parameters, while the least-squares method is in the backward path to identify the consequent parameters. As a result, the nonlinear relationship between  $\eta(n(t))$  and  $n(t)$  is identified and thus producing an estimate  $\hat{\eta}$  in the output. Instead of suppressing the interference  $\eta(t)$  from the primary channel, the ANFIS operation takes  $\hat{g}$  as a contaminated version of  $\eta(t)$  in the primary channel for training. Further inside into the ANFIS operation and its process layers can be found in [9].

- TM-levelization: Its functionality is to generate a dynamic level-based process controlled by two gauges as depicted in Fig. 1(b):  $TM_{\alpha_1}$ , the external gauge and  $TM_{\alpha_2}$ , the internal gauge. As the TM-levelization process slides through the ANC output, the  $TM_{\alpha_1}$  is set iteratively up. Its task is to generate loops that keep updating the optimum TME scheme, removing power of most of the sharp detail information in the sense of trimmed mean estimation, and to achieve fast convergence towards an optimal target mapping in the CWT operation. With  $TM_{\alpha_1}$  being set, the internal gauge  $TM_{\alpha_2}$  is operated iteratively down to preserve the potentials arisen from the previous mapping, i.e. the data trimmed percentage rate goes down. When the level of  $TM_{\alpha_1}$  increases, more peaks of similar level to the contact signal become revealed. At the same time, decreasing the level of  $TM_{\alpha_2}$  results in less and less power of potentials being removed in order to preserve the contact signal. Note that when the proceeded signal has a strong target strength, the TM step can be skipped to increase the process speed of the TME scheme. This setting can be always done at the first iteration of the TME scheme.
- WDeN: The wavelet denoising operation is designed to further suppress the noise part of the training data followed by the TM step or resulted from the ANC scheme by applying the thresholding rule to the detail coefficients. This operation is proven to be efficient and can be viewed as a nonparametric estimation of the desired noise-free signal [14]. The de-noising procedure proceeds in three steps:
  - 1) Decomposition: Choose a wavelet, and specify a level N. Compute the wavelet decomposition of the signal at the level N.
  - 2) Detail coefficients thresholding: For each level from 1 to N, select a threshold and apply thresholding rule to the detail coefficients.
  - 3) Reconstruction: Compute wavelet reconstruction based on the original approximation coefficients of the level N and the modified detail coefficients of levels from 1 to N.

## III. SIMULATION RESULTS

### A. Input data description for ANC neuro-fuzzy scheme

In the ANC neuro-fuzzy scheme illustrated in Fig. 1(a), four channels of interference signal corresponding to the returns from 16 pings of 1s duration, delivered in complex format, together with the same number of contact signal, are used to form the primary and reference inputs to the ANC scheme.

TABLE I  
CRITICAL PARAMETERS SETTING.

Sonar Environment Setting	Sea Depth (m)	100
	Sonar Depth (m)	50
	Wind Speed	6 m/s( $\approx$ sea state 3)
	Seabed Type	Medium Sand
	Number of Beams	1
	Beamwidth	3dB ( $\approx$ 40 degrees)
	Maxi. Target Range (m)	500
Synthetic Echo Environment Setting	Pulse	Morlet Wavelet
	Pulse Length (ms)	2
	Echo Duration (s)	1
	Sampling Frequency (Hz)	100k
	Amplitude ( $\alpha_i$ )	0.1
	SNR range (dB)	[-30,0]
ANFIS Environment Setting	Data Set per Source	2
	MFs per Input	4
	MF Type	Gaussian
	Input-Output Data Load	100k
TM Level Setting	Training/Checking Rate	[50%, 50%]
	Basic Step Range	$[0.15, 0.75] \times 10^{-3}$
DWT Denoise Setting	Increment Percentage	60%
	Wavelet Type	Daubechies 10
	Decomposition Level	16
CWT Mother Wavelet Setting	Threshold Type	Soft
	Wavelet Type	Morlet Wavelet
	Support Range	[-5, 5]
	Scale Range	[25, 36]
	Filter Tap Range	[250, 360]

More specifically, as depicted in synthetic echo setting of Table I, the contact signal is the mother wavelet in the CWT mapping and is adopted as Morlet wavelet [2]

$$\psi(t) = \exp(-\alpha t^2) \exp(j2\pi f_c t). \quad (15)$$

The waveform consists of a window function governed by  $\alpha = 9.5657 MHz$  and a modulation function adjusted by  $f_c = 20 kHz$ , a central frequency of the waveform. In the following evaluations, the 16 pings of returns are based on the various levels of the target strength in the range  $SNR = [-30, 0] db$ . In addition, four channels of interference signal include the first two channels with reverberation  $\mathbf{r}$  and white Gaussian noise  $\mathbf{n}$  mixed together in each channel. This constitutes the major source of interference signal for the input of unknown corrupting channel of noise path filter I ( $\hat{h}_1$ ) and yields the output  $\eta_{\mathbf{r}+\mathbf{n}}$ . The remaining two channels contain solely the white Gaussian noise with zero mean and variance 0.04 to feed into the corrupting channel of noise path filter II ( $\hat{h}_2$ ) and also yields the output  $\eta_{\mathbf{n}}$ . The channels of noise path filters are to simulate the worse detectable situation in highly distorting media. For simplicity but still representing an extreme case of the classical tests, channels of noise path filter are chosen as follows:

$$\begin{aligned} \hat{h}_1(x_1, x_2) &= 50(x_1 + x_2) + 100 \\ \hat{h}_2(x_1, x_2) &= 50(x_2 - x_1^2)^2 + (1 - x_1)^2. \end{aligned} \quad (16)$$

Input data of ANFIS de-noise operation as given in the ANFIS setting of Table I includes four Gaussian memory functions (MFs) on each of the two input-output training pairs. Due to the sampling frequency of the returns, there are totally 100k input-output data pair. Among them 50% of the data set is taken for the training modes, while the remaining 50% is for the checking modes to validate the identified fuzzy model.

TABLE II  
COMPARISON BETWEEN IDEAL OUTPUTS AND THE TME OUTPUTS.

Synthetic echo Algorithm Output	$T_1$		$T_2$	
	Ideal	TME	Ideal	TME
TOA (s)	.25	.254813	.60	.5995
Location(pts)	25585	25582	60060	60056
Acceleration ( $m/s^2$ )	35	34.4706	-.05	-.1256
Initial velocity (kn)	20.0		-1.0	
Final Velocity (kn)	37.7037	37.7032	-1.05067	-1.05066

### B. Input data description for the TME scheme

The input data for the optimum TME scheme is listed in Table I. In the step of TM-levelization, it contains 5 basic level set up empirically within the range  $[0.15, 0.75] \times 10^{-3}$  and being updated with an increase of 60%. In the step of wavelet decomposition, different levels of target strength can be viewed by using a unique mother wavelet. In all examples presented here, the largest scale level is set to be 16 and the orthogonal mother wavelet is empirically chosen as the Daubechies extremal phase wavelet [10] of order 10. Soft threshold is adopted for the mother wavelet to yield minimax performance for mean square error against an ideal procedure. The CWT mother wavelet is adopted by the Morlet wavelet as described in Eq. (15) with the duration of  $2ms$ . The waveform is sampled at  $32Hz$  with effective support  $[-5, 5]$  for the lowest level of similarity measurement within the scale range  $[25, 36]$ . The resultant signal is then split into FIR filter banks with the tap range  $[250, 360]$ .

### C. Results

Together with the real data set supported by DERA UK as part of the torpedo homing research programme, we evaluate the performance of the proposed hybrid algorithm for two scenarios of the multiple targets' motion estimation. As illustrated in Table I for the sonar environment, there were 16 data sets received for various target strength. Furthermore, the strength of signal to reverberation is measured by the target's echo to reverberation waveform.

1) *Scenario I*: This scenario is to estimate target's Doppler motion (radial range, velocity and acceleration) at the signal strength of  $SNR=-30db$  for two targets' ping noted by  $T_1$  and  $T_2$ . More specifically, the ping  $T_1$  is from a sonar guided modern torpedo (such as the spearfish torpedo) launched below the surface by a submarine. The torpedo's mission is to search for and home in its target with the ping  $T_2$ . The torpedo is thus assumed moving away from the signal receiver with initial speed based on its parent vehicle, and its radial acceleration is calculated at the moment when it is firing. The pinged target  $T_2$  is assumed almost stationary with slow motion towards the signal receiver. Detail of both targets are listed in the table II. Combined with the four input channels received together with the noise path filters all depicted in Figs. 2(a)-(f), the complex signal is obtained and depicted in Fig. 3(c), while Fig. 3(a)-(b) are given for reference. As can be viewed clearly, pings  $T_1$  and  $T_2$  are completely buried in the background interference. By the setting of initial parameters given in Table I, Figs. 4(a) and 5(a) show the output of ANC neuro-fuzzy scheme with

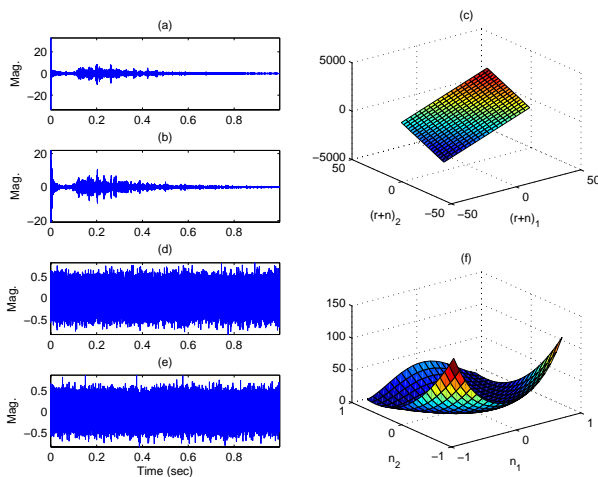


Fig. 2. Interference sources. (a)-(b): Reverberation waveforms  $r_1$  and  $r_2$ . (c): Unknown corrupting linear channel of NPF for reverberation. (d)-(e): White Gaussian waveforms  $n_1$  and  $n_2$  with zero mean and variance 0.04. (f): Unknown corrupting nonlinear channel of NPF for white Gaussian noise.

5 epochs of ANFIS operation employed for training and validating the complex signals. Performing the first WDeN of the optimum TME scheme yields outputs given in Fig. 4(b) for echo  $T_1$  and Fig. 5(b) for echo  $T_2$ . Followed by the optimal CWT similarity measurement, the estimated location of ping  $T_{1e}$  as depicted in Fig. 4(c) is accurately matched to the ideal ping  $T_1$  with 3 sampling points difference. While, a false alarm occurred in Fig. 5(c) for  $T_2$  is due to its weak returned signal as can be viewed by Fig. 3(a). As a result, the first level of TM-levelization with the gauge level  $TM_{\alpha_1} = TM_{\alpha_2} = 7.5 \times 10^{-4}$  is performed to get rid of excessive noise and yields the 2<sup>nd</sup> WDeN output shown in Fig. 5(d). Performing the optimal CWT measurement, the location of  $T_2$  is successfully pinged at  $T_{2e}$  with 4 sampling points difference as illustrated in Fig. 5(e).

2) *Scenario II*: This scenario is to consider various levels of the target strength in the range  $SNR = [-30, 0]db$  with 2db element spacing for the estimation of total 16 echo returns. Here each return contains two pings of target signal,  $T_1$  and  $T_2$ . Statistical results in the sense of the normalized absolute error (NAE) and the relative absolute error (RAE) will be used to examine the performance of the hybrid algorithm. To efficiently implement the hybrid algorithm, the range of ANFIS epoch in the ANC-neuro scheme is set based on 6 different ranges of SNR. That is, for the ranges of SNR level  $[-5(k+1), -5k-1]db$ ,  $k = 0, \dots, 5$ , their corresponding iterations are set at  $2 \leq [1.5k/2]$ ,  $k = 1, \dots, 6$  epoches. Figs. 6(a)-(e) and 7(a)-(e) show prediction errors of target motion parameters in terms of NAE of the  $T_1$  and  $T_2$  targets, respectively. In all 16 trials, clearly each estimate of parameter has accurately matched their corresponding correct ones with the maximum false detection of 1.5%. In addition, the overall error measurements of RAE as can be seen in Fig. 6(f) and 7(f) of each target parameters are also about 1.5% false detection rate. Fig. 8 demonstrates the computational efficiency of the hybrid algorithm in dealing with both targets in various target

strength with average cost of 31.476 sec per trial.

#### IV. CONCLUSION

In this contribution, the ANC-TME hybrid algorithm developed previously for real-time applications in FPGA hardware implementation was examined to evaluate its performance by real data set given. Its excellent performance indicated by the simulation has been shown to be suitable for the detection of underwater targets' Doppler motion at very low target strength. Quantitative analyses of the performance evaluation obtained for each returns of ping have even shown that the hybrid algorithm not only meets the development requirements but also provides a higher degree of signal detection capability with an increased robustness against false signal detections.

#### ACKNOWLEDGMENT

This work acknowledges the technical support by DERA (UK) and the financial support by NSC (Taiwan) under grant no.: NSC 98-2221-E-168-028.

#### REFERENCES

- [1] R. Young, Wavelet Theory and Its Applications, Kluwer Academic Publisher, Boston, 1993.
- [2] L. G. Weiss, "Wavelets and wideband correlation processing," *IEEE Signal Processing Magazine*, pp. 13-32, 1994.
- [3] H. Naparst, "Dense target signal processing," *IEEE Trans. Inform. Theory*, vol. 37, pp. 317-327, 1991.
- [4] P. Delaney and D. Walsh, "Performance analysis of the incoherent and skewness matched filter detectors in multioath environments," *IEEE Journal of Oceanic Engineering*, vol. 20, no. 1, pp. 80-84, 1995.
- [5] C. H. Tseng and M. Cole, "Towards smart-pixel-based implementation of wideband active sonar echolocation system for multi-target detection," ICSPCS2008, Gold Coast, Australia, 2008.
- [6] C. H. Tseng, and M. Cole, "Optimum multi-target detection using an ANC neuro-fuzzy scheme and wideband replica correlator," *IEEE ICASSP2009*, pp. 1369-1372, Taipei, Taiwan.
- [7] C. H. Tseng, "Effective wideband acoustic sonar signal detection based on adaptive neuro-fuzzy processor and optimal wavelet transform," The 17th National Conference on Fuzzy Theory and Its Application, pp. 817-822, Kaohsiung, 2009.
- [8] B. Widrow et al., "Adaptive noise cancelling: Principles and applications," *IEEE proc.*, vol. 63, pp. 1692-1716, 1975.
- [9] J-S R. Jang, C. T. Sun, and E. Mizutani, Neuro-Fuzzy and Soft Computing: A Computational approach to learning and machine intelligence. Pearson Education Taiwan Ltd, 2004.
- [10] S. Mallat, A Wavelet Tour of Signal Processing, 2/e, Academic Press, UK, 1999.
- [11] R. P. Brent, Algorithms for Minimization without Derivatives, Prentice-Hall, Englewood Cliffs, New Jersey, 1973
- [12] M. A. Mansour, B. V. Smith, and J. A. Edwards, "PC-based real-time active sonar simulator," *IEE Proc.-Radar, Sonar Navig.*, vol. 144, pp. 227-233, 1997.
- [13] M. Sugeno, "Industrial applications of fuzzy control," Elsevier Science Pub. Co., 1985.
- [14] D. L. Donoho, "De-Noising by soft-thresholding," *IEEE Trans. on Inf. Theory*, vol. 41, 3, pp. 613-627, 1995.

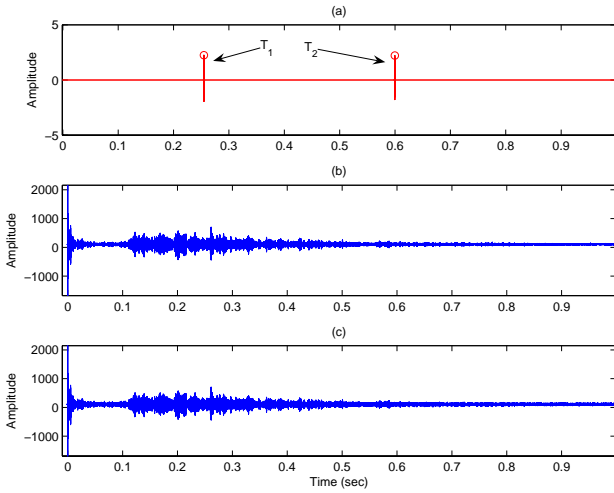


Fig. 3. Time-domain received signal echoes. (a)Noise-free synthetic echoes:  $T_1$  and  $T_2$ . (b)Additive Interference consisting of reverberation of Morlet and WGN(0,0.04) sampled at 100 kHz. (c)Composite returned signal with the target strength SNR= $-30dB$ .

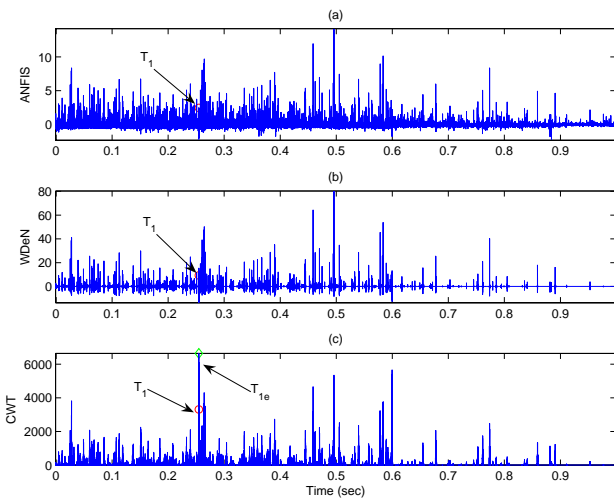


Fig. 4. (a)ANC neuro-fuzzy output of the 1<sup>st</sup> target ping  $T_1$  with 5 ANFIS epochs. (b)Output of the 1<sup>st</sup> WDeN without TM-levelization. (c) Output of the 1<sup>st</sup> optimal CWT mapping:  $|f^3(s_1^*) - f^0(s_1^*)|$ .

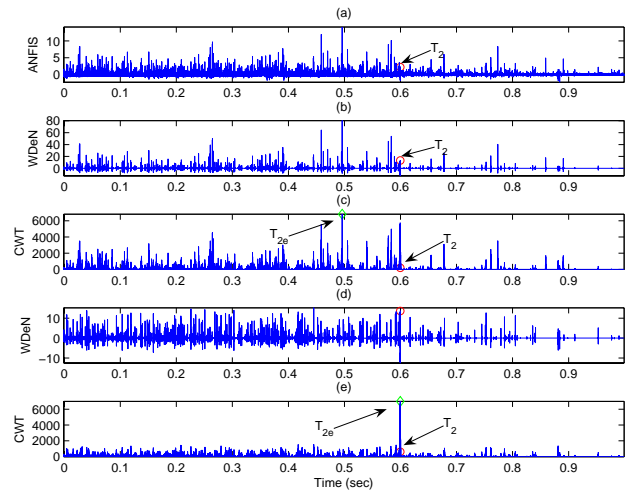


Fig. 5. (a)ANC neuro-fuzzy output of the 2<sup>nd</sup> target ping  $T_2$  with 5 ANFIS epochs. (b)Output of the 1<sup>st</sup> WDeN without TM-levelization. (c) Output of the 1<sup>st</sup> optimal CWT mapping:  $|f^3(s_1^*) - f^0(s_1^*)|$ . (d) Output of the 2<sup>nd</sup> WDeN with  $TM_{\alpha_1} = TM_{\alpha_2} = 7.5 \times 10^{-4}$ . (e) Output of the 2<sup>nd</sup> optimal CWT mapping:  $|f^3(s_2^*) - f^0(s_2^*)|$ .

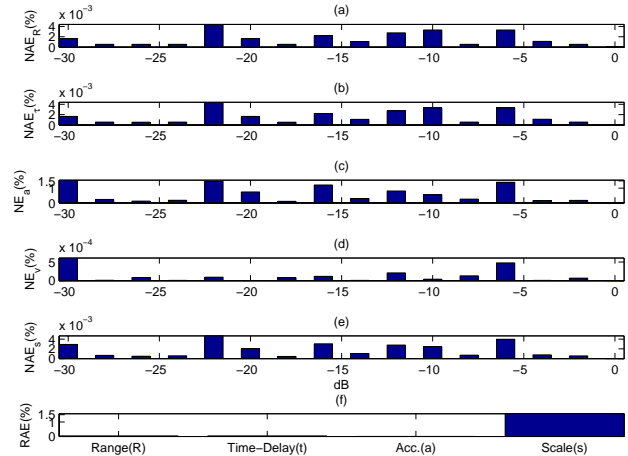


Fig. 6. Performance evaluation using NAE (%) and RAE (%) for  $T_1$  at the SNR range of  $[-30, 0]dB$ : (a)NAE range. (b)NAE round-trip time-delay ( $\tau$ ). (c)NAE radial acceleration (a). (d)NAE Doppler scale (s). (e)RAE motion parameters

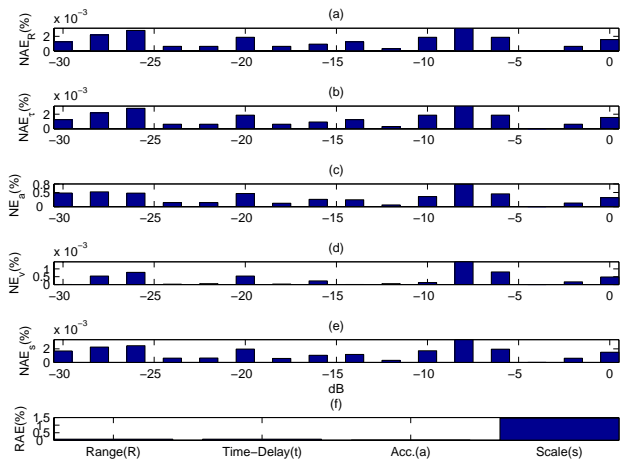


Fig. 7. Performance evaluation using NAE (%) and RAE (%) for  $T_2$  at the SNR range of  $[-30, 0]dB$ : (a)NAE range. (b)NAE round-trip time-delay ( $\tau$ ). (c)NAE radial acceleration (a). (d)NAE Doppler scale (s). (e)RAE motion parameters

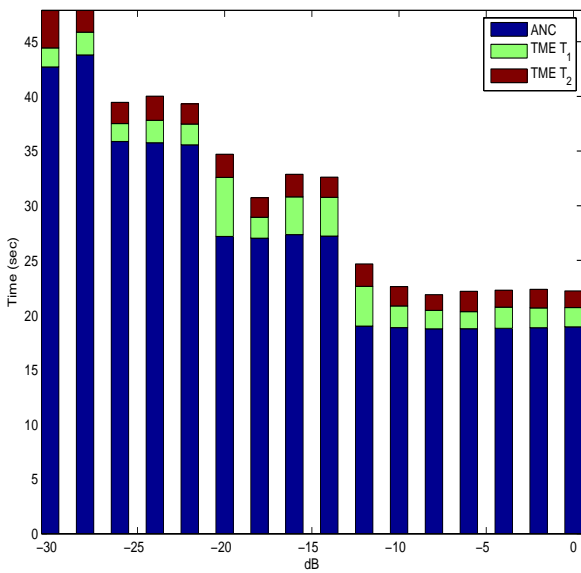


Fig. 8. Computational time consumption for the detection of  $T_1$  and  $T_2$  at the SNR range of  $[-30, 0]dB$  with average cost of 31.476 sec/trial.